The discharge coefficient - experimental measurement of a dependence on density contrast

Gary R. Hunt‡ & Joanne M. Holford

Department of Applied Mathematics and Theoretical Physics,

Silver Street, University of Cambridge, CB3 9EW, UK.

Synopsis

At sufficiently high Reynolds numbers, the discharge coefficient C_d associated with a sharply contracting flow through a square-edged opening is, in general, taken to be constant. The effect of buoyancy forces, due, for example, to temperature differences between the air on either side of the opening, is ignored.

We hypothesise that the buoyancy force may result in a significant *reduction* in the discharge coefficient associated with the flow through a square-edged opening in a horizontal surface. We test this hypothesis by deducing C_d from laboratory measurement of the two-layer stratification produced by a localised buoyancy source in an enclosure which ventilates passively in a displacement mode. Experiments were performed at small scale in a water tank using saline solutions to generate buoyancy forces.

In the absence of a buoyancy contrast, the discharging flow contracts due to inertial effects giving $C_d \approx 0.6$. In the presence of a buoyancy contrast, our results show that the discharge through a horizontal vent takes the form of a rising plume-like flow, which may contract further giving a smaller value of C_d. The plume-like discharge is characterised by conditions at the discharge opening, which we represent by a single dimensionless parameter Γ_d - the *discharge parameter*. Our results demonstrate that once a critical value of Γ_d is exceeded, C_d exhibits a strong dependence on the density contrast and rapidly decreases with increasing Γ_d. The implications of a dependence of C_d on density contrast are for potentially serious errors in the prediction of airflow rates if a constant value of C_d is assumed.

List of Symbols

A^*	effective opening area of ventilated enclosure (m^2)
A_{vc}	cross-sectional area of discharging jet at the *vena contracta* (m^2)
A_1 , A_2	cross-sectional area (m^2),
	pipe flow application: $_1$ of approach duct, $_2$ of opening in duct;
	ventilation application: $_1$ of enclosure, $_2$ of discharge opening
b_{min}	minimum radius of plume-like discharge, *i.e.* at height of max. contraction (m)
b_0	initial radius of plume-like discharge, $= 5Q_d/6\alpha M_d^{1/2}$ (m)
C_d	discharge coefficient
D_{vc}	hydraulic diameter of jet at the *vena contracta* (m)
D_1 , D_2	hydraulic diameter (m),
	pipe flow application: $_1$ of approach duct, $_2$ of opening in duct;
	ventilation application: $_1$ of enclosure, $_2$ of discharge opening

‡ present address: Department of Civil & Environmental Engineering, Imperial College of Science, Technology and Medicine, LONDON, SW7 2BU, UK.

g	acceleration due to gravity (ms^{-2})
g_d'	reduced gravity of buoyant layer in enclosure and, thus, of the discharge (ms^{-2})
$h^* = H-h$	depth of buoyant layer in enclosure (m)
H	vertical distance between buoyancy source and discharge opening (m)
L	length of internal face of discharge opening parallel to flow axis (m)
Q_a , Q_t	actual volume flow rate, volume flow rate predicted by ideal flow theory (m^3s^{-1})
Q_d , M_d , B_d	volume flux (m^3s^{-1}), momentum flux (m^4s^{-2}), buoyancy flux (m^4s^{-3}) at the discharge opening
Q_p , g_p' , B_p	initial volume flow rate (m^3s^{-1}), initial reduced gravity (ms^{-2}) and initial buoyancy flux (m^4s^{-3}) of the source supplying buoyancy to the enclosure
Re	Reynolds number at the discharge opening
T_0	reference temperature (°K)
u	characteristic velocity at discharge opening
z	vertical co-ordinate (m)
Γ_d	discharge parameter
Δp	pressure drop across discharge opening ($kg\ m^{-1}s^{-2}$)
ΔT_d	temperature difference between fluid on either side of the discharge opening (°K)
$\Delta\rho_d$	initial density contrast between discharging fluid and ambient fluid ($kg\ m^{-3}$)
ε	surface roughness (m)
λ	area ratio, = area of discharge opening / area of approach duct
μ , ν	viscosity ($kg\ m^{-1}s^{-1}$), kinematic viscosity (m^2s^{-1}),
ρ_0 , ρ_d	density of ambient fluid, density of fluid discharged ($kg\ m^{-3}$)
ϕ	area ratio, = minimum cross-sectional area of discharging flow / A_2

1. Introduction

The passage of air through even the simplest building typically requires the flow to contract suddenly in order to pass through a ventilation opening and following the contraction there is usually an expansion, *e.g.* when air is discharged through a ventilation opening into the atmosphere. Flows through contractions and expansions are encountered in many engineering applications, most commonly in pipe flows, and are well documented (Batchelor[1], Ward-Smith[2], Idelchik[3]). In building ventilation, the details of the flow through the opening are of secondary interest while the primary interest is the volume flow rate of air through the opening.

General features of flow through an opening

For sufficiently high Reynolds numbers† (above 4000, Ward-Smith[2]) the flow through a sharp-edged opening has the same general features regardless of the details of the opening geometry. The flow accelerates as it enters the opening (area A_2) and continues to contract for a distance downstream, to a minimum cross-sectional area A_{vc} at the so-called *vena contracta* (*vc*), see figure 1a. The flow is laminar in the region of flow convergence between the

† Etheridge & Sandberg[4] (pg.77) tabulate typical Reynolds numbers Re encountered in practice for openings in low and high rise buildings and as a guide give $300 \lesssim Re \lesssim 600{,}000$, where $Re = uD_2/\nu_a$, u is a characteristic velocity at the opening, D_2 the hydraulic diameter of the opening and ν_a the kinematic viscosity of air. The quoted range of Re is based on pressure differences of 10 Pa and 60 Pa in the low and high rise buildings, respectively.

opening and the *vc*, while downstream of the *vc* a transition to turbulence occurs as the flow is decelerated by an adverse pressure gradient. The degree of contraction ϕ ($= A_{vc} / A_2$) depends on the geometric details of the opening and in particular on: i) the geometry of the upstream edge of the opening (*e.g.* whether sharp-edged or smoothly rounded), ii) the length L of the internal face of the opening parallel to the flow axis, and iii) the ratio $\lambda = A_2 / A_1$ of the cross-sectional areas of the approach duct (hydraulic diameter D_1 and area A_1) and the discharge opening (hydraulic diameter D_2 and area A_2).

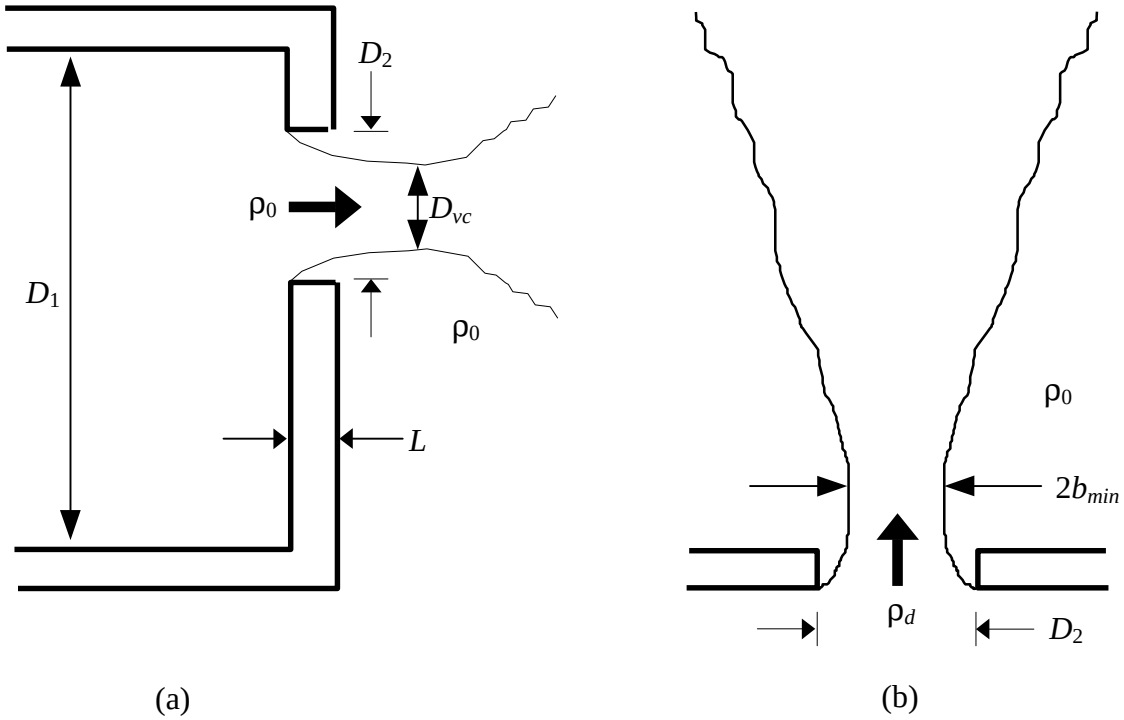

Figure 1. Schematics showing: (a) general features of the flow through an opening in the absence of a density contrast (D_{vc} denotes the hydraulic diameter of the jet at the *vena contracta*), and (b) flow contraction in a rising thermal plume formed by buoyant fluid discharging through an opening. The density contrast $\Delta\rho_d = \rho_0 - \rho_d$, $(\rho_0 > \rho_d)$; b_{min} denotes the minimum radius of the plume-like discharge, *i.e.* the radius at the height of maximum contraction. The heavy arrow indicates the direction of flow through the opening.

The discharge coefficient

The discharge coefficient C_d may be regarded as the ratio of the actual flow rate Q_a , found by measurement in a real flow, to the flow rate Q_t predicted by idealised inviscid flow theory:

$$C_d = \frac{Q_a}{Q_t}. \qquad (1)$$

Idealised flow theory (Batchelor[1]) reveals the dependence of the flow rate on the opening area A_2 and the magnitude of the pressure drop Δp across the opening. Assuming that the velocity profile across the opening is uniform and that there is no subsequent contraction

$$Q_t = A_2 \sqrt{2\Delta p / \rho_0}\ , \qquad (2)$$

where ρ_0 denotes the fluid density. The *actual* flow rate will depend additionally on the fluid viscosity μ, surface roughness ε of the opening and the area ratio λ:

$$Q_a = f(A_2, \Delta p, \mu, \rho_0, \lambda, \varepsilon), \tag{3}$$

where $f(\,)$ denotes 'some function of '. On dimensional grounds we expect

$$\frac{Q_a}{A_2\sqrt{2\Delta p/\rho_0}} = f(Re, \lambda, \frac{\varepsilon}{D_2}) \equiv C_d\,. \tag{4}$$

At this stage, and as is shown in (4), the unknown function f of Re, λ and ε/D_2 is termed the discharge coefficient. For certain opening geometries, further theoretical progress has been made in expressing C_d in terms of the flow quantities, however, these analyses still draw on an empirical constant. For example, in the absence of surface roughness, Ward-Smith[2] expresses C_d as

$$C_d = \left[\phi^2(1-\lambda^2)/(1-\phi^2\lambda^2)\right]^{1/2}, \tag{5}$$

where ϕ is determined empirically. Measurements of flow through square-edged openings with $L/D_2 \ll 1$ (*e.g.* Ward-Smith[2], pg.395) show that the degree of jet contraction decreases as the area of the opening approaches the area of the approach duct (*i.e.* ϕ increases as λ increases), although, the net effect is an approximately constant value of C_d. In fact, $C_d \approx 0.6$ over the wide range of area ratios $\lambda \lesssim 0.7$ (Ward-Smith[2], pg.392). For extremely sharp contractions, *i.e.* in the limit as $\lambda \to 0$, (5) reduces to $C_d = \phi$ (≈ 0.6, according to measurement).

These principles of pipe flow are traditionally applied to building ventilation as a means of estimating the discharge coefficient for a ventilation opening. There are measurements which support the use of $C_d \approx 0.6$ for flows through openings in buildings (*e.g.* Flourentzou, Mass & Roulet[5]) and others, *e.g.* Aynsley, Vickery & Melbourne[6] and Heiselberg, Svidt & Nielsen[7], which indicate that use of a constant value could lead to significant errors in flow rate predictions.

The analogy between the ventilation opening and the pipe constriction is not always appropriate as, for example, unlike flow in a pipe, air flow may be deflected over and around the building, and the geometry of ventilation openings are typically far more complex than flow constrictions (*e.g.* circular 'orifice plates') commonly encountered in pipes. In addition, previous studies have focused primarily on the discharge of a single fluid of uniform density through openings, again in the context of contractions in pipe flows. In many cases of practical interest, including ventilation flows, fluid of one density may flow through an opening into a region of fluid of a different density, *e.g.* when warm air flows through an upper opening of a heated room into the (cooler and denser) outside air. The presence of these buoyancy forces is, however, usually assumed to have a negligible effect.

Recent measurements of discharge coefficients in a laboratory test room by Heiselberg, Svidt & Nielsen[7] for various vertical window openings indicate that this may be a considerable oversimplification. Their measurements of C_d varied between approximately 0.8 and 1 depending on the window type (whether bottom hung, side hung or a combination), opening area and temperature difference.

Enhanced flow contraction due to buoyancy forces

In this paper we restrict our attention to the discharge of (warm) fluid upwards through a horizontal opening into a region of (cool) fluid of contrasting density. Owing to the density contrast, the flow discharging from the opening will be plume-like as it rises. Studies on turbulent plumes (Morton[8], Caulfield[9], Hunt & Kaye[10]) demonstrate that a plume may contract as it rises above the source (figure 1b). The plume contraction is a result of the initial acceleration of the fluid as it leaves the opening and is entirely due to the action of the buoyancy forces, although, it may be regarded as being analogous to the *vena contracta* formed in the absence of buoyancy forces. The degree of plume contraction depends on the initial plume conditions, *i.e.* conditions at the discharge opening, and in particular on the area of the opening, the volume flow rate and the density contrast. The buoyancy-induced contraction may be significantly greater (see §2) than the inertial contraction for flows of a single density where the maximum contraction corresponds to $\phi \approx 0.6$.

With this in mind, we hypothesise that in the presence of a density contrast the plume-like discharge will have a significant effect on the discharge characteristics of the opening and may yield $C_d < 0.6$. In order to test this hypothesis, a series of experiments were conducted and the dependence of the discharge coefficient on the source conditions of the plume-like discharge deduced. Experiments were conducted in water tanks using salt solutions to create density contrasts. Before describing the experiments, we appeal to plume theory for further insight.

2. Theoretical considerations - when do thermal plumes contract ?

The development of the rising turbulent plume, which results from a discharge of buoyant fluid (of density ρ_d) into a fluid of constant density ρ_0 may be characterised in terms of the fluxes of volume Q_d , buoyancy B_d (or heat) and momentum M_d from the discharge opening. These fluxes may be combined and expressed as a dimensionless parameter

$$\Gamma_d = \delta \frac{{Q_d}^2 B_d}{{M_d}^{5/2}}, \tag{6}$$

(see Morton[8], Hunt & Kaye[10]), where $\delta = 5/(2^{7/2}\alpha\pi^{1/2})$ is dependent on the plume entrainment coefficient α (≈ 0.083). If we assume a uniform velocity profile across the opening then (6) reduces to

$$\Gamma_d = \delta \frac{{A_2}^{5/2} g_d'}{{Q_d}^2} = \delta \frac{{A_2}^{5/2} g \Delta T_d}{{Q_d}^2 T_0}, \tag{7}$$

as $B_d = Q_d\, g_d'$. The reduced gravity is $g_d' = g\Delta\rho_d / \rho_0$, where $\Delta\rho_d = \rho_0 - \rho_d$ denotes the density contrast between the discharging fluid and the surrounding environment. For an ideal fluid $g_d' = g\Delta T_d / T_0$, where ΔT_d denotes the temperature contrast across the opening and T_0 a reference temperature (°K). The importance of Γ_d is in representing the balance between buoyancy and inertial effects at the discharge opening. In the absence of buoyancy $\Gamma_d = 0$, and as buoyancy effects become increasingly dominant so Γ_d increases. We refer to Γ_d hereafter as the *discharge parameter*.

Theoretical predictions♣ plotted in figures 2 and 3 show the effect of Γ_d on the development of the buoyant plume-like discharge as it rises above the opening. Figure 2 shows the plume radius as a function of height z for a range of Γ_d. For $\Gamma_d < 2.5$ the plume expands continuously as it rises. For $\Gamma_d = 2.5$ the plume is straight-sided close to the source (*i.e.* for small z the plume's radius remains approximately constant) and it expands in radius as it rises higher. For $\Gamma_d > 2.5$ the rising plume contracts immediately above the source to a minimum radius b_{min} before then increasing in radius as it rises higher. Caulfield[9] deduces theoretically that plumes contract, or 'neck', close to their source providing $\Gamma_d > 2.5$. As Γ_d increases further, the contraction increases. This can be confirmed by reference to figure 3 which plots the variation of the minimum plume radius b_{min} with Γ_d.

It is the effect of the contracting plume on the discharge characteristics of the opening that is of interest here. To examine the influence of the plume contraction on the discharge coefficient, a series of laboratory experiments were performed. These are now described.

3. Experiments

Two series of experiments were performed. The first series examined how the discharge properties of an opening vary as a layer of buoyant fluid drains from an enclosure under a displacement mode of ventilation; a situation representative of a space night cooling. In the second series, a single discharge coefficient was deduced for each of a range of steady two-layer stratifications established by a localised buoyancy source in an enclosure with displacement ventilation. In this paper we report only on the latter steady flow experiments.

The experimental configuration was quite simple. A clear Perspex container of rectangular cross section was immersed in a larger environmental tank filled with fresh water. The top of the container was fully open and one or more circular openings were made in the base. Table 1 gives the dimensions of the container, base opening areas and area ratios considered. Buoyancy (salt solution) was supplied to the container from a localised source positioned a height H above the base. The experimental set-up is depicted in figure 4. Saline solution of reduced gravity g_p' was supplied at a constant flow rate Q_p. The resulting descending saline plume formed a layer of dense salt solution at the base of the container, below a layer of fresh water, and drove a displacement flow. Fresh water was drawn in through the top of the container and salt solution drained out through one or more openings in the base. After an initial transient period, the saline layer attained a steady depth $h^* = H\text{-}h$ and uniform steady reduced gravity g_d' . The depth h^* was measured to within 1 mm and the reduced gravity to an accuracy of 5 x 10^{-3} gcm^{-3} using an Anton Paar density meter.

By varying the height H (see Appendix B for limitations) of the source above the base, a range of different steady density stratifications and, hence, different discharge parameters Γ_d , were produced. The discharge coefficient associated with that stratification was then deduced (Appendix C) using

$$C_d = \frac{Q_p g_p'}{\sqrt{2} A_2 g_d'^{3/2} \sqrt{(H - h + z_v)}} . \qquad (8)$$

♣ The predictions shown in figures 2 and 3 are solutions of the plume conservation equations (Appendix A) subject to the classical entrainment assumption (Morton, Taylor and Turner[11]).

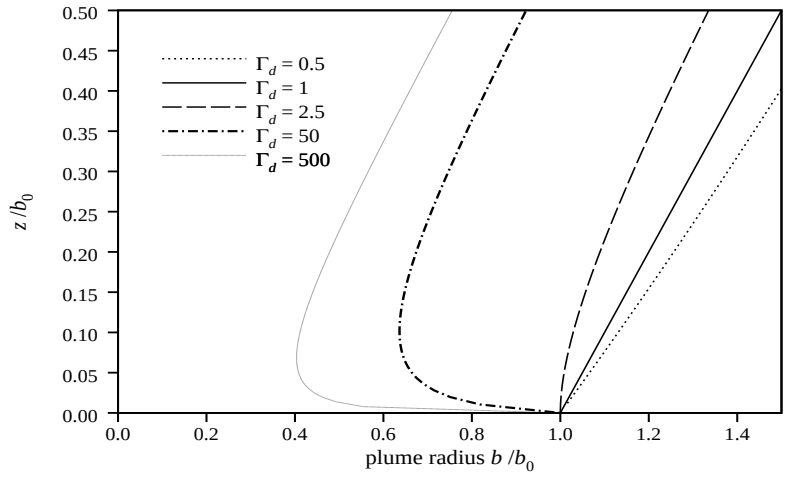

Figure 2. Plume radius $b(z)/b_0$ as a function of height z/b_0 for discharge parameters Γ_d = 0.5, 1, 2.5, 50 and 500. Note that for $\Gamma_d < 2.5$ the radius increases with height; for $\Gamma_d = 2.5$ the plume is straight-sided before increasing in radius; for $\Gamma_d > 2.5$ the plume contracts before increasing in radius.

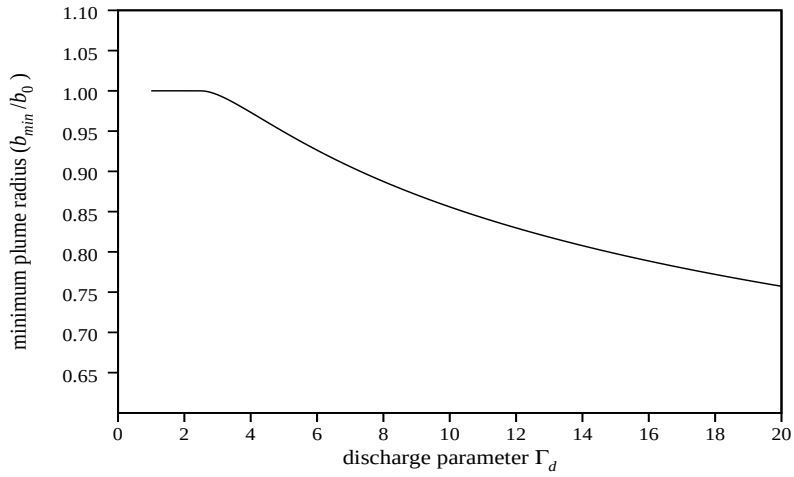

Figure 3. The minimum plume radius b_{min}/b_0 *vs*. the discharge parameter Γ_d. Note that for $\Gamma_d < 2.5$ no contraction occurs. For $\Gamma_d > 2.5$, b_{min} decreases as Γ_d increases, *i.e.* the plume contraction is more pronounced (see, also Morton & Middleton[12]).

	Single opening A_2 = 23.76 cm^2	Two openings A_2 = 47.52 cm^2
Box #1 (A_1 = 40cm x 40cm)	1/67	1/34
Box #2 (A_1 = 30cm x 20cm)	1/25	1/13

Table 1. Approximate area ratios $\lambda = A_2/A_1$ for the two containers and two discharge opening areas considered in the steady flow experiments. Discharge openings were circular with square edges; D_2 = 5.5 cm and L = 1 cm. A_1 and A_2 are the cross-sectional areas of the container and discharge opening, respectively.

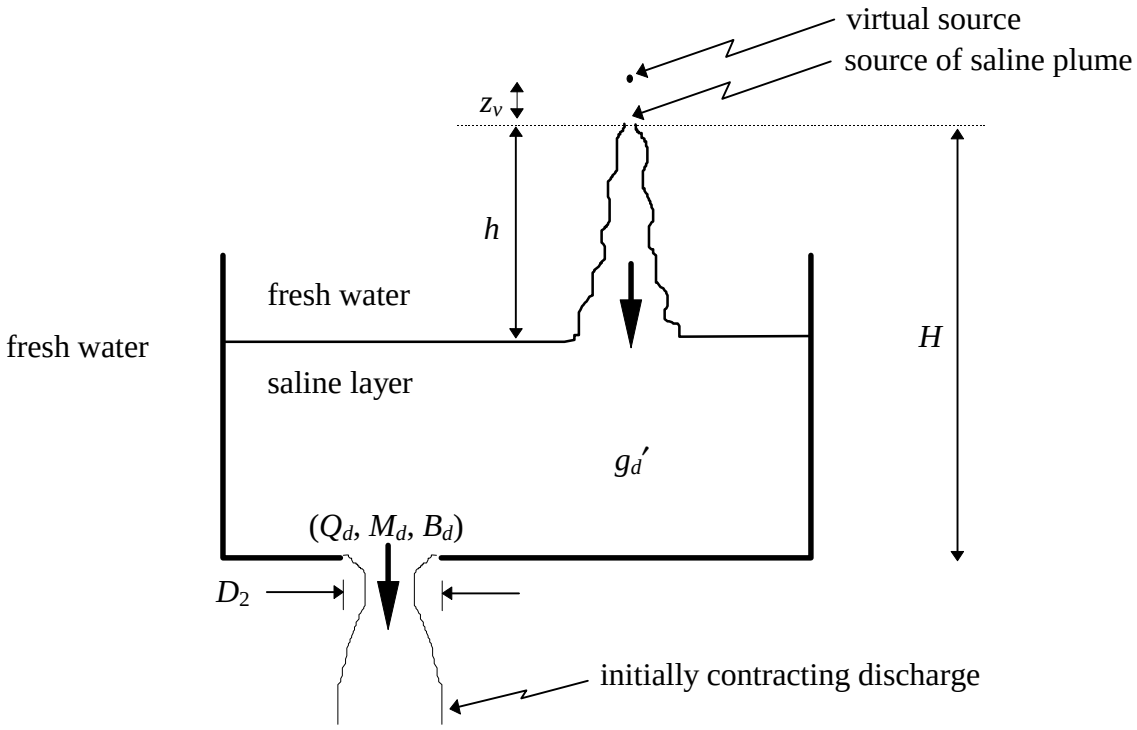

Figure 4. Schematic showing the experimental set-up. The buoyancy source was positioned a height H above the base of the container. The steady depth $H–h$ and reduced gravity g_d' of the saline layer were measured for a range of different H.

4. Results

Discharge coefficients deduced from the laboratory measurements are plotted as a function of Γ_d in figure 5. The dependence of C_d on Γ_d is clear and dramatic; for small Γ_d (or, equivalently, small density contrasts) C_d decreases relatively slowly with increasing Γ_d, whereas for larger Γ_d (larger density contrasts) the rate of decrease of C_d with Γ_d increases. Note that an increase in the density contrast corresponding to an increase in Γ_d from 0 to 40 results in a decrease in C_d of over 40 %. A best fit♠ to the data yields the empirical formula

$$C_d = 0.71 - 1.9\text{x}10^{-4}\Gamma_d{}^2, \qquad \text{for } 0 \le \Gamma_d \le 40. \tag{9}$$

The empirical fit suggests $C_d \approx 0.7$ in the absence of a density contrast (*i.e.* when $\Gamma_d = 0$); this value is consistent with existing measurements for openings with $L/D_2 \approx 1/5$.

For $\Gamma_d \lesssim 10$, figure 5 shows that the discharge coefficient depends weakly on Γ_d and the traditional assumption, namely, that the buoyancy force has a negligible effect on the discharge coefficient, is valid. For larger Γ_d , the discharge coefficient varies strongly with increasing Γ_d and the assumption of a constant value of C_d would clearly be in error. Reynolds numbers *Re* corresponding to the data shown in figure 5 are shown in figure 6. For

♠ A fit of the quadratic form (9) is justified on the grounds that for small density contrasts we expect, and observe, a weak dependence of C_d on Γ_d . In fact, for $\Gamma_d < 2.5$ we predict (figure 2) no additional contraction over the *vena contracta* formed by inertial effects due to the action of buoyancy forces. An appropriate fit should therefore exhibit the behaviour $dC_d/d\Gamma_d = 0$ at $\Gamma_d = 0$, which, indeed, (9) does.

$\Gamma_d \gtrsim 20$, C_d exhibits a rapid decrease with increasing Γ_d (figure 5) while the Reynolds number remains approximately constant (figure 6). This indicates that the reduction in C_d is due to the change in Γ_d and not *Re*.

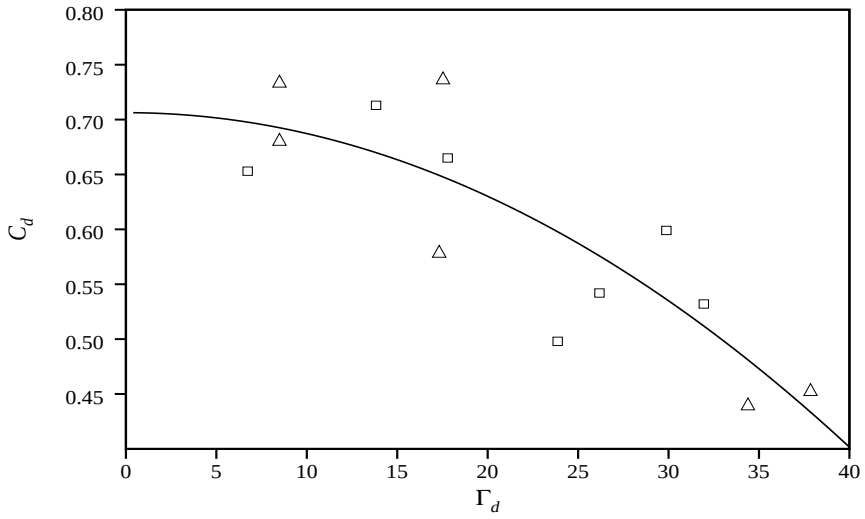

Figure 5. Discharge coefficient C_d *vs*. discharge parameter Γ_d . Data is marked as Δ for a single opening, for two openings. The curve represents the best fit (9). Experiments were conducted for $6 < \Gamma_d < 40$. For the experiments shown, $1700 \lesssim Re \lesssim 3100$.

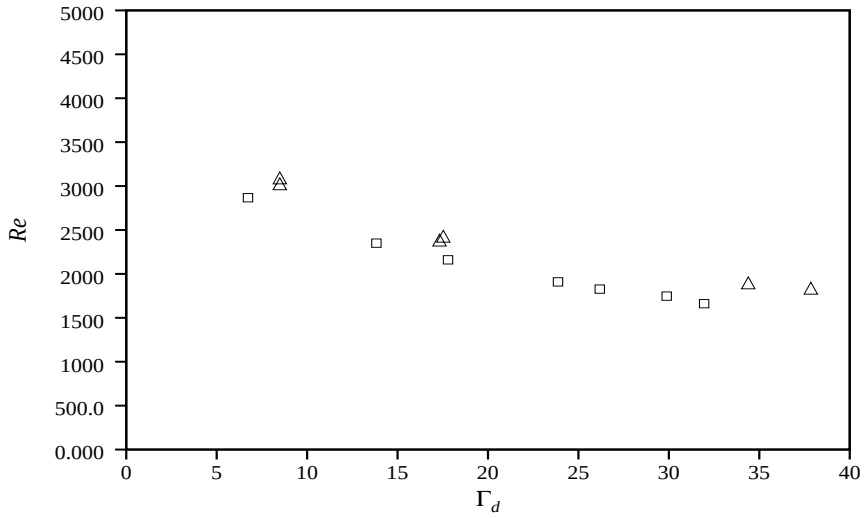

Figure 6. Reynolds number *Re* at the discharge opening *vs*. discharge parameter Γ_d . Data is marked as Δ for a single opening, for two openings. $Re = 4Q_d / \pi D_2 \nu_w$, where ν_w denotes the kinematic viscosity of water ($\nu_w = 0.01\ cm^2 s^{-1}$) and $Q_d = B_p\, g_d'$.

5. Implications

With reference to the definition of the discharge parameter (7) we note that large values of Γ_d can be achieved by making:

- the discharge opening area A_2 large
- the temperature contrast ΔT_d large, or
- the volume flow rate Q_d small,

(with all other quantities fixed in each case). Thus, highly buoyant, low velocity discharges from large openings give large values of Γ_d and, hence, discharge coefficients significantly lower than those associated with flows through openings in the absence of a density contrast.

6. Conclusions

The discharge coefficient C_d associated with the flow through a sharp-edged circular opening has been measured for a range of density (or equivalently, temperature) differences across the opening. Our attention has focused on horizontal openings.

Our measurements show that the discharge coefficient is dependent on the temperature difference across the discharge opening and that large contrasts in temperature may *reduce* the discharge coefficient significantly.

We observe that a discharge of buoyant fluid from a horizontal opening produces a plume-like flow, which may contract considerably in cross section as it rises. This contraction effectively further reduces the useable area of the opening and gives rise to reduced values of the discharge coefficient. We characterise the extent of the contraction by a dimensionless parameter - the discharge parameter Γ_d - which provides a measure of the relative importance of buoyancy and inertia at the opening. Highly buoyant, low velocity releases from large area openings give large values of Γ_d and large contractions.

For small values of Γ_d , buoyancy effects are weak and discharge coefficients appropriate for flows in the absence of a density contrast are suitable for estimating airflow rate.

As Γ_d increases, *e.g.* due to an increase in the opening area or the temperature difference and reduction in the volume flow rate, buoyancy effects become increasingly important. The discharge coefficient is now shown to depend on Γ_d and, hence, on the density contrast. A key implication to building ventilation is that use of a 'traditional' discharge coefficient for predicting airflow rates through horizontal openings will result in a significant over-prediction when $\Gamma_d \gg 1$.

Acknowledgements

GRH & JMH acknowledge the financial support of the EPSRC and the Leverhulme Trust. We would like to thank B. Dean, D. Lipman, C. Mortimer, D. Page-Croft and L. Pratt for their craftmanship and technical support in the laboratory.

References

1.BATCHELOR, G.K.
"An introduction to fluid dynamics"
Cambridge University Press, 1967, 615 pp.

2.WARD-SMITH, A.J.
"Internal fluid flow - the fluid dynamics of flow in pipes and ducts"
Oxford, 1980, 566 pp. Oxford Science Publications, Clarenden Press.

3.IDELCHIK, I.E.
"Handbook of hydraulic resistance"
1986, Hemisphere Publishing, Washington, D.C.

4.ETHERIDGE, D.W. and SANDBERG, M.
"Building Ventilation: Theory and Measurement"
John Wiley & Sons Ltd., Chichester UK, 724 pp. 1996. ISBN 047196087.

5.FLOURENTZOU, F., MASS, J. VAN DER and ROULET, C.A.
"Experiments in natural ventilation for passive cooling"
Proceedings of the 17th AIVC Conference, Gothenburg, Sweden, 1996, 121—134.

6.AYNSLEY, R.M., MELBOURNE, W. and VICKERY, B.J.
"Architectural Aerodynamics"
Applied Science Publishers Ltd., 1977, London. ISBN: 0-85334-698-4. 254pp.

7.HEISELBERG, P., SVIDT, K. and NIELSEN, P.V.
"Windows - measurements of air flow capacity."
Proceedings of Roomvent 2000, Reading, UK, July 9-12th. Ed. H.B. Awbi. Elsevier Science Ltd. 2000, **2**, 749—754. ISBN 0-080-43017-1.

8.MORTON, B. R.
"Forced plumes"
J. Fluid Mech. **5**, 1959, 151—163.

9.CAULFIELD, C.P.
"Stratification and buoyancy in geophysical flows"
PhD thesis, 1991, University of Cambridge, UK.

10.HUNT, G.R. and KAYE, N.G.
"Virtual origin correction for lazy turbulent plumes"
Submitted for publication *J. Fluid Mech*. 2000.

11.MORTON, B. R., TAYLOR, G. I. and TURNER, J. S.
"Turbulent gravitational convection from maintained and instantaneous sources"
Proc. Roy. Soc. **234**, 1956, 1—23.

12.MORTON, B. R. and MIDDLETON, J.
"Scale diagrams for forced plumes"
J. Fluid Mech. **58**, 1973, 165—176.

13.LINDEN, P.F., LANE-SERFF, G.F. and SMEED, D.A.
"Emptying filling boxes: the fluid mechanics of natural ventilation"
1990, *J. Fluid Mech.*, **212**, 300-335.

Appendix A - Solution of the plume equations

Assuming Gaussian profiles for vertical velocity and buoyancy and an unstratified quiescent environment, the plume equations for conservation of volume, momentum and buoyancy, under the Boussinesq approximation, may be written in the form

$$\frac{dQ}{dz} = 2^{3/2}\pi^{1/2}\alpha M^{1/2}, \qquad \frac{dM}{dz} = \frac{QB}{M} \qquad \text{and} \qquad \frac{dB}{dz} = 0, \qquad (10, 11, 12)$$

respectively, see Morton, Taylor & Turner (1956)[11], where, $Q(z)$, $M(z)$ and B denote the fluxes of volume, momentum and buoyancy. For an extended forced plume, the source conditions are $Q = Q_d$, $M = M_d$ and $B = B_d$ at $z = 0$. (12) expresses that the buoyancy flux is conserved in an unstratified environment, hence, $B(z) = const. = B_d$. Scaling the variables in the plume on the source conditions, we introduce the non-dimensional quantities $m = M/M_d$, $q = Q/Q_d$ and $B/B_d = 1$. The vertical co-ordinate z is scaled on the initial plume radius $b_0 = 5Q_d /6\alpha M_d^{1/2}$. Solution of (10 - 12) yields the integral equation

$$\frac{z}{b_0} = \frac{3}{5\pi^{1/2}2^{1/2}}\Gamma^{-1/5}\int_1^q \left(q^2 - \frac{\Gamma_d - 1}{\Gamma_d}\right)^{-1/5} dq\,. \qquad (13)$$

The numerical solution of (13) is plotted in figures 2 and 3. The dimensionless plume radius $b(z)/b_0 = q/m^{1/2}$.

Appendix B - Limitations on the range of experiments: selective withdrawal

The range of stratifications from which the discharge coefficient was determined (§3) was limited to those for which *only* saline solution flowed out through the lower opening. If the saline layer produced is sufficiently shallow then the interface is no longer horizontal but 'bows' down towards the opening and fluid from both saline and fresh water layers (of densities ρ_d and ρ_0, respectively) is discharged through the opening. At this stage the opening is no longer 'selective' as it allows fluids of both densities to pass through.

Appendix C - Deducing C_d from experimental measurement of two-layer stratification

From experimental measurement of the steady layer depth $h^* = H–h$ and reduced gravity g_d' produced by a localised buoyancy source (a saline plume), of initial buoyancy flux $B_p = Q_p\, g_p'$, located a height H above the base of an enclosure operating in a displacement mode, the discharge coefficient for the outlet opening was deduced as follows. The volume flow rate driven by the saline layer is given by $Q_d = A^*(g_d' h^*)^{1/2}$, see Linden, Lane-Serff & Smeed[13], where the effective opening area A^* reduces to

$$A^* = \sqrt{2}C_d A_2 \qquad (c1)$$

when the inlet opening area is significantly larger than the outlet (discharge) opening area. Substituting for A^* into the expression for Q_d we obtain

$$C_d = \frac{Q_d}{\sqrt{2}A_2\sqrt{g_d' h^*}}\,. \qquad (c2)$$

Before C_d can be determined, it is necessary to determine Q_d. This can be achieved as buoyancy is conserved, *i.e.* in the steady state, the buoyancy flux B_p supplied via the saline plume must be identical to the buoyancy flux B_d discharged through the outlet, so $B_p = Q_p\, g'_p = Q_d\, g_d' = B_d$ and, hence, $Q_d = Q_p\, g_p'/g_d'$. Thus

$$C_d = \frac{Q_p g'_p}{\sqrt{2}A_2 g_d'^{3/2}\sqrt{h^*}}\,. \qquad (c3)$$

After accounting for the virtual origin location (see figure 4, and Hunt & Kaye[10]), (c3) is modified to give (8).